

Search for Two-Photon Production of Resonances Decaying into $K\bar{K}$ and $K\bar{K}\pi$

TASSO Collaboration

M. Althoff, W. Braunschweig, F.J. Kirschfink,
H.-U. Martyn, R. Rosskamp, H. Siebke¹, W. Wallraff
I. Physikalisches Institut der RWTH Aachen, D-5100 Aachen,
Federal Republic of Germany¹¹

J. Eisenmann, H.M. Fischer, H. Hartmann,
A. Jocksch, G. Knop, H. Kolanoski, H. Kück²,
V. Mertens, R. Wedemeyer

Physikalisches Institut der Universität Bonn, D-5300 Bonn,
Federal Republic of Germany¹¹

B. Foster, A. Wood

H.H. Wills Physics Laboratory, University of Bristol,
Bristol BS8 1TL, UK¹²

E. Bernardi, Y. Eisenberg³, A. Eskreys⁴, K. Gather,
H. Hultschig, P. Joos, B. Klima, H. Kowalski,
A. Ladage, B. Löhr, D. Lüke, P. Mättig⁵,
G. Mikenberg³, D. Notz, D. Revel³, D. Trines,
T. Tymieniecka⁶, R. Walczak⁶, G. Wolf, W. Zeuner

Deutsches Elektronen-Synchrotron, DESY, D-2000 Hamburg 52,
Federal Republic of Germany

E. Hilger, T. Kracht, H.L. Krasemann,
E. Lohrmann, G. Poelz, K.U. Pösnecker

II. Institut für Experimentalphysik der Universität Hamburg,
D-2000 Hamburg, Federal Republic of Germany¹¹

D.M. Binnie, P.J. Dornan, D.A. Garbutt, C. Jenkins,
W.G. Jones, J.K. Sedgbeer, D. Su, J. Thomas,
W.A.T. Wan Abdullah⁷

Department of Physics, Imperial College,
London SW7 2AZ, UK¹²

Received 29 August 1985

F. Barreiro⁸, L. Labarga, E. Ros
Universidad Autonoma de Madrid, Madrid, Spain¹⁵

M.G. Bowler, P. Bull, R.J. Cashmore, P. Dauncey,
R. Devenish, C.M. Hawkes, G. Heath, D.J. Mellor
Department of Nuclear Physics, Oxford University,
Oxford OX1 3RH, UK¹²

S.L. Lloyd
Department of Physics, Queen Mary College,
London E1 4NS, UK¹²

K.W. Bell, G.E. Forden, J.C. Hart, D.K. Hasell,
D.H. Saxon

Rutherford Appleton Laboratory, Chilton, Didcot,
Oxon OX11 0QX, UK¹²

S. Brandt, M. Dittmar¹⁰, M. Holder, G. Kreutz,
B. Neumann

Fachbereich Physik der Universität-Gesamthochschule Siegen,
D-5900 Siegen, Federal Republic of Germany¹¹

E. Duchovni¹⁰, U. Karshon, A. Montag, R. Mir,
E. Ronat, G. Yekutieli, A. Shapira

Weizmann Institute, Rehovot 76100, Israel¹³

G. Baranko, A. Caldwell, M. Cherney,
M. Hildebrandt, J.M. Izen, M. Mermikides, S. Ritz,
D. Strom, M. Takashima, H. Venkataramania⁹,
E. Wicklund, S.L. Wu, G. Zobernig

Department of Physics, University of Wisconsin,
Madison, WI 53706, USA¹⁴

¹ Now at DEC, Hamburg, FRG

² Now at Fraunhofer Institut, Duisburg, FRG

³ On leave from Weizmann Institute, Rehovot, Israel

⁴ On leave from Institute of Nuclear Physics, Cracow, Poland

⁵ Now at IPP Canada, Carleton University, Ottawa, Canada

⁶ On leave from Warsaw University, Poland

⁷ On leave from University of Malaya, Kuala Lumpur

⁸ Now at University of Siegen, FRG

⁹ Now at Yale University, New Haven, CT, USA

¹⁰ Now at CERN, Geneva, Switzerland

¹¹ Supported by the Bundesministerium für Forschung und Technologie

¹² Supported by the UK Science and Engineering Research Council

¹³ Supported by the Minerva Gesellschaft für Forschung mbH

¹⁴ Supported by the US Department of Energy, contract DE-AC02-76ER00881 and by the US National Science Foundation Grant Number INT-8313994 for travel

¹⁵ Supported by CAICYT

Abstract. An analysis of the production of $K_S^0 K_S^0$ and $K^\pm K_S^0 \pi^\mp$ by two quasi-real photons is presented. The cross section for $\gamma\gamma \rightarrow K^0 \bar{K}^0$, which is given for the $\gamma\gamma$ invariant mass range from $K\bar{K}$ threshold to 2.5 GeV, is dominated by the $f'(1525)$ resonance and an enhancement near the $K\bar{K}$ threshold. Upper limits on the product of the two-photon width times the branching ratio into $K\bar{K}$ pairs are given for $\Theta(1700)$, $h(2030)$, and $\xi(2220)$. For exclusive two-photon production of $K^\pm K_S^0 \pi^\mp$ no significant signal was observed. Upper limits are given on the cross section of $\gamma\gamma \rightarrow K^+ \bar{K}^0 \pi^-$ or $K^- K^0 \pi^+$ between 1.4 and 3.2 GeV and on the product of the $\gamma\gamma$ width times the branching ratio into the $K\bar{K}\pi$ final states for the $\eta_c(2980)$ and the $\iota(1440)$, yielding $\Gamma(\gamma\gamma \rightarrow \iota(1440)) \cdot \text{BR}(\iota(1440) \rightarrow K\bar{K}\pi) < 2.2 \text{ keV}$ at 95 % C.L.

1. Introduction

Two-photon production of resonances with even C -parity can be studied at e^+e^- colliding beam machines in the process

$$e^+e^- \rightarrow e^+e^- + R. \quad (1)$$

In this process the resonance R is produced by two predominantly quasi-real photons which are radiated by both leptons. For a given $\gamma\gamma$ helicity state and with the restriction to quasi-real photons the only unknown parameter in reaction (1) is the two-photon partial width $\Gamma_{\gamma\gamma}(R)$.

In the past the two-photon widths of the pseudoscalar mesons π^0 [1], η , η' and of the tensor mesons $f(1270)$, $A_2(1320)$ and $f'(1525)$ were measured [2, 3]. Recently also the two-photon production of the scalar meson $\delta(980)$ was reported [2].

Measurements of two-photon widths probe the charge content of mesons. Since in the framework of the quark model mesons differ in their composition of quarks with different charges, the knowledge of the coupling to two photons provides a test of $SU(3)$ symmetry and the determination of the singlet-octet mixing angle for the flavour neutral members of a $SU(3)$ multiplet. In conjunction with information on resonances obtained from other reactions (in particular radiative decays), the measured two-photon widths were used to search for exotic (non- $q\bar{q}$) states. For instance, the abundant two-photon production of $\rho^0\rho^0$ below 2 GeV [3] has been interpreted as the production of four-quark states [4]. Bound states of gluons, glueballs, being composed of neutral constituents, are naively expected to be characterized by small $\gamma\gamma$ widths. Glueball candidates as observed in radiative J/ψ decays are the $\iota(1440)$ [5], $\Theta(1700)$

[6] and the $\xi(2220)$ [7]. A measurement of the $\gamma\gamma$ coupling of these states is very important for an assessment of their gluonic nature.

2. Data Taking

In this paper we report on cross section measurements and a search for resonances in the reactions

$$e^+e^- \rightarrow e^+e^- K_S^0 K_S^0 \rightarrow e^+e^- \pi^+ \pi^- \pi^+ \pi^- \quad (2)$$

and

$$e^+e^- \rightarrow e^+e^- K^\pm K_S^0 \pi^\mp \rightarrow e^+e^- K^\pm \pi^+ \pi^- \pi^\mp. \quad (3)$$

The experiment was performed with the TASSO detector at the e^+e^- storage ring PETRA. A description of the detector can be found elsewhere [8]. In case of reaction (2) the data were taken at beam energies mainly around 17.5 GeV and correspond to an integrated luminosity of 83.3 pb^{-1} . For reaction (3) the integrated luminosity amounts to 74.8 pb^{-1} collected at an average beam energy of 16.95 GeV.

Events were recorded if they fulfilled at least one of the following trigger conditions:

1. four or more charged tracks in the central tracking chambers,
2. any two charged tracks having associated signals in the inner time-of-flight counters separated by more than 154° in azimuth,
3. two or more charged tracks originating from the interaction region.

These triggers were based on the central proportional and drift chamber processors, which required the track momenta perpendicular to the beam, $|\mathbf{p}_t|$, to exceed preselected nominal values. This leads to momentum dependent track detection efficiencies which for most of the data vary from 50 % at $|\mathbf{p}_t| = 0.17 \text{ GeV}$ to about 95 % at $|\mathbf{p}_t| > 0.29 \text{ GeV}$.

3. Event Selection

The final states of reaction (2) and (3) are both composed of four charged hadrons. The detection of the scattered electrons was not required. In the analyses presented here only the information from the central wire chambers and the surrounding inner time-of-flight counters was used. Event candidates for reaction (2) and (3) were selected by requiring exactly four charged tracks in the central wire chambers with net charge zero. All tracks had to have $|\mathbf{p}_t| > 0.1 \text{ GeV}$ and $|\cos \Theta| < 0.87$ (Θ is the polar angle of the track relative to the beam axis). In order to reject one-photon annihilation events the sum of the track momenta was required to be $\sum |\mathbf{p}| < 8.0 \text{ GeV}$.

At that point of the analysis chain 38,959 events were left. The further cuts applied to reduce the data sample are different for reaction (2) and (3).

4. Analysis

4.1. The Reaction $\gamma\gamma \rightarrow K_S^0 K_S^0$

In order to suppress events with additional undetected particles the net transverse momentum of the hadronic system was required to be $|\sum \mathbf{p}_t| \leq 0.120$ GeV, leaving 6,134 events. This cut also restricts the two photons to be dominantly quasi-real. In the analysis of reaction (2) all detected particles were assumed to be pions. For the identification of the neutral kaons the $\pi^+\pi^-$ invariant mass spectra were used. No attempt was made to search for the secondary decay vertex of the K_S^0 mesons since this method yields too small efficiencies at the low kaon momenta considered in this analysis. Figure 1a shows the invariant mass of one $\pi^+\pi^-$ pair plotted versus the invariant mass of the other $\pi^+\pi^-$ pair (2 entries per event). Besides a broad bump in the $\rho^0\rho^0$ region a cluster of events in the $K_S^0 K_S^0$

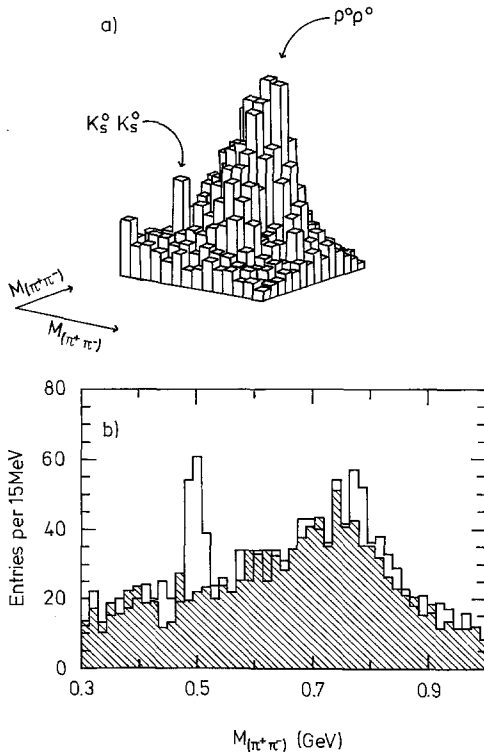


Fig. 1. **a** Invariant mass of one $\pi^+\pi^-$ pair vs. the invariant mass of the other one in events with four charged tracks (2 entries per event). **b** Invariant mass of one $\pi^+\pi^-$ pair if the other one lies in the K_S^0 signal band (unshaded histogram) or if the other one lies in the background region (shaded histogram); (up to 4 entries per event)

region is observed. In Fig. 1b the unshaded histogram shows the invariant mass of one $\pi^+\pi^-$ pair if the other one lies in the K_S^0 region defined by $|m_{K_S^0} - m_{\pi^+\pi^-}| < 0.025$ GeV (up to 4 entries per event are possible), whereas the shaded histogram shows the corresponding averaged distribution for the $\pi^+\pi^-$ combinations lying in the two sidebands defined by $|(m_{K_S^0} \pm 0.050 \text{ GeV}) - m_{\pi^+\pi^-}| < 0.025$ GeV. The signal in the unshaded histogram indicates production of $K_S^0 K_S^0$ pairs.

Candidate events for two-photon produced $K_S^0 K_S^0$ pairs have to fulfill the condition

$$R_{KK} \equiv \sqrt{(m_{(\pi^+\pi^-)_1} - m_{K_S^0})^2 + (m_{(\pi^+\pi^-)_2} - m_{K_S^0})^2} < 0.025 \text{ GeV}$$

for at least one of the two possible combinations of two neutral pion pairs $(\pi^+\pi^-)_1$ and $(\pi^+\pi^-)_2$. This condition is fulfilled by 72 events with invariant masses between the $K\bar{K}$ threshold and 2.5 GeV. The histogram in Fig. 2a shows the $K_S^0 K_S^0$ mass distribution of these events. The background curve (full line) is determined from events lying in a ring around the $K_S^0 K_S^0$ region with $0.043 \text{ GeV} \leq R_{KK} \leq 0.050 \text{ GeV}$.

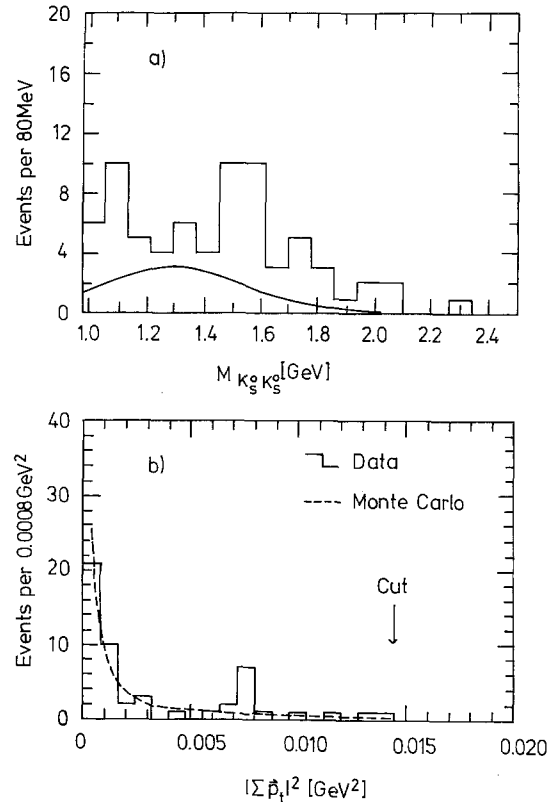


Fig. 2. **a** Event yield in the $K_S^0 K_S^0$ signal region (unshaded histogram) as a function of the $K_S^0 K_S^0$ invariant mass. The full line shows the background contribution. **b** $|\sum \mathbf{p}_t|^2$ distribution of the background subtracted $K_S^0 K_S^0$ event yield (histogram) compared to the corresponding Monte-Carlo prediction (dashed line)

This method of background determination has been checked by varying the size and position of the background area. After background subtraction $51 \pm 9 K_S^0 K_S^0$ events are left.

The background corrected $|\sum \mathbf{p}_i|^2$ distribution of the $K_S^0 K_S^0$ events is shown in Fig. 2b. The peak at $|\sum \mathbf{p}_i|^2 \approx 0$ indicates exclusive production of $K_S^0 K_S^0$. The dashed line in Fig. 2b shows the corresponding $|\sum \mathbf{p}_i|^2$ distribution for the Monte-Carlo simulation of reaction (2) which is in qualitative agreement with the data. The background of events with additional undetected particles is about $20\% \pm 4\%$ and was subtracted.

In the Monte-Carlo simulation of reaction (2) the events were generated according to:

$$\frac{d\sigma_{e^+e^- \rightarrow e^+e^-x}}{dW_{\gamma\gamma} d\omega d\xi} = \frac{dL(W_{\gamma\gamma}, \omega)}{dW_{\gamma\gamma} d\omega} \cdot F(q_1^2, q_2^2) \cdot \frac{d\sigma_{\gamma\gamma \rightarrow x}(W_{\gamma\gamma}, \xi)}{d\xi},$$

where ω represents the kinematical variables of the two-photon system other than $W_{\gamma\gamma}$, the invariant mass of the hadronic final state X , while ξ represents the kinematical variables of the four particles of the system X . For $L(W_{\gamma\gamma}, \xi)$, which is the flux of transverse photons, we used the exact formula from [9]. The function $F(q_1^2, q_2^2)$ contains the dependence on the photon four-momenta q_i^2 and has been parametrized as ρ pole form factors. The Monte-Carlo events were analysed in the same way as the data.

In Fig. 3 we show the cross section σ for the reaction $\gamma\gamma \rightarrow K^0 \bar{K}^0$. The event rates are corrected for $K_L^0 K_L^0$ production and the unseen decay modes of the K_S^0 . Apart from an enhancement at the $K^0 \bar{K}^0$ threshold the main contributions to the cross section are seen in the $W_{\gamma\gamma}$ region of the tensor mesons

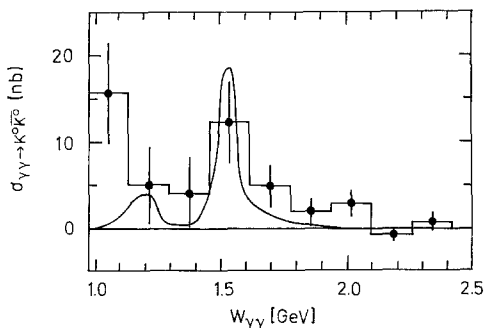


Fig. 3. Total cross section $\sigma(\gamma\gamma \rightarrow K^0 \bar{K}^0)$ as a function of $W_{\gamma\gamma}$. The curve corresponds to a coherent superposition of the three relativistic Breit-Wigner amplitudes of the $f(1270)$, $A_2(1320)$, and $f'(1525)$ as described in the text

$f(1270)$, the $A_2(1320)$, and especially the $f'(1525)$. Thus we simulated the $K^0 \bar{K}^0$ production by using an angular distribution with spin $J=2$ and helicity $\lambda=2$ for $W_{\gamma\gamma} \geq 1.14$ GeV. The cross section in the threshold bin of Fig. 3 is calculated using S -wave production of the $K^0 \bar{K}^0$ pairs in the Monte-Carlo simulation. Using an isotropic angular distribution, instead of a distribution with spin $J=2$ and $\lambda=2$, increases the cross section below 1.14 GeV only by 10% while at higher $W_{\gamma\gamma}$ the cross section is increased by 40%. The curve in Fig. 3 shows the contribution of the tensor mesons $f(1270)$, $A_2(1320)$, and $f'(1525)$ to the cross section $\sigma(\gamma\gamma \rightarrow K^0 \bar{K}^0)$. It results from a coherent superposition of the three Breit-Wigner amplitudes as explained in [10] using previously determined values for the $\gamma\gamma$ couplings to these resonances. In the $K^0 \bar{K}^0$ final state the isoscalar $f(1270)$ and the isovector $A_2(1320)$, which are nearly mass degenerate, interfere destructively [11]. This explains why no resonance peak is seen in the $f(1270)$ and the $A_2(1320)$ region. The errors are statistical only, the systematic errors decrease from 25% at the $K\bar{K}$ threshold to about 10% at $W_{\gamma\gamma} \geq 1.5$ GeV. Above 2.1 GeV no $K^0 \bar{K}^0$ signal is observed.

Special attention was given to the threshold behavior of the cross section to find indications for scalar resonance production. The angular distribution below 1.14 GeV is consistent with S -wave production of $K_S^0 K_S^0$ pairs, but limited statistics do not allow to draw final conclusions.

The two-photon coupling of the $f'(1525)$ has been presented in an earlier publication by the TASSO collaboration analysing the same data with a slightly different method [10]. The $\gamma\gamma$ width times the branching ratio into $K\bar{K}$ pairs was determined by taking into account the interference of the relativistic Breit-Wigner resonance amplitudes of the $f(1270)$, the $A_2(1320)$, and the $f'(1525)$. As can be seen from the curve in Fig. 3 the present analysis is consistent with the previously quoted result of $\Gamma(\gamma\gamma \rightarrow f'(1525)) \cdot \text{BR}(f'(1525) \rightarrow K\bar{K}) = (0.11 \pm 0.02 \text{ (stat.)} \pm 0.04 \text{ (syst.)}) \text{ keV}$.

In the energy region above the $f'(1525)$ we observe no significant indication for contributions from resonances decaying into $K\bar{K}$. Therefore upper limits on the product of the $\gamma\gamma$ width times the branching ratio into $K\bar{K}$ pairs can be derived for the $\theta(1700)$ which has spin-parity $J^P=2^+$ [6], the $h(2030)$ which has $J^P=4^+$ [12], and the recently observed state $\xi(2220)$ [7]. The upper limits are derived by fitting relativistic Breit-Wigner resonance curves to the measured event rates and are given for $K\bar{K}$ production (i.e. the acceptance has been calculated including all possible charge combinations of

$K\bar{K}$ pairs). The uncertainties in the resonance parameters used have been taken into account.

In the fit of $\Theta(1700)$ we used as mass $m_\Theta=(1.720\pm 0.010)\text{ GeV}$ and width $\Gamma_\Theta=(0.130\pm 0.020)\text{ GeV}$ [6]. The $\Theta(1700)$ was fitted in the $W_{\gamma\gamma}$ region between 1.64 GeV and 1.85 GeV. The tail of the $f'(1525)$ was taken into account. From the fit we derived an upper limit on the product of the $\gamma\gamma$ width times the branching ratio into $K\bar{K}$ of $\Gamma(\gamma\gamma\rightarrow\Theta(1700))\cdot\text{BR}(\Theta(1700)\rightarrow K\bar{K})<0.28\text{ keV}$ (95 % C.L.). For the acceptance calculations of the $\Theta(1700)$ we assumed the spin-parity assignment $J^P=2^+$ with helicity $\lambda=2$. If $\lambda=0$ is assumed, the upper limit increases by a factor of two.

Mass and width of the $h(2030)$ are $m_h=(2.027\pm 0.012)\text{ GeV}$ and $\Gamma_h=(0.220\pm 0.030)\text{ GeV}$ [12]. We fitted a Breit-Wigner resonance curve for the $h(2030)$ between 1.82 GeV and 2.2 GeV. The fit gave an upper limit on the product of the $\gamma\gamma$ width times the branching ratio into $K\bar{K}$ pairs of $\Gamma(\gamma\gamma\rightarrow h(2030))\cdot\text{BR}(h(2030)\rightarrow K\bar{K})<0.29\text{ keV}$ (95 % C.L.). The upper limit for the $h(2030)$ was determined with the spin-parity assignment $J^P=4^+$ and holds for helicity $\lambda=0$ and $\lambda=2$.

Preliminary results for mass and width of the $\xi(2220)$ are $m_\xi=(2.237\pm 0.013)\text{ GeV}$ and $\Gamma_\xi=(0.021\pm 0.030)\text{ GeV}$ [7]. The mass resolution of the TASSO detector in this range is $\sigma_{\text{mass}}\approx 0.025\text{ GeV}$. In the $W_{\gamma\gamma}$ region between 2.1 GeV and 2.35 GeV one event is observed. From that we derived an upper limit of $\Gamma(\gamma\gamma\rightarrow\xi(2220))\cdot\text{BR}(\xi(2220)\rightarrow K\bar{K})\cdot(2J+1)<1.0\text{ keV}$ (95 % C.L.). The spin-parity of the $\xi(2220)$ has not yet been measured. The upper limit holds for both spin-parity $J^P=0^+$ and $J^P=2^+$ with helicity $\lambda=0$ and $\lambda=2$.

4.2. The Reaction $\gamma\gamma\rightarrow K^\pm K_S^0\pi^\mp$

We now turn to the analysis of reaction (3) which is also based on the sample of events defined in Sect. 3. For the identification of charged kaons the information provided by the 48 inner time-of-flight (TOF) scintillation counters surrounding the central tracking chambers was used. The TOF analysis was only done for tracks in a polar angular range $|\cos\Theta|<0.8$ to be well within the acceptance of the TOF counters. For efficient separation between pions, kaons and protons the momentum of these tracks had to be in the range $0.3\text{ GeV}<|\mathbf{p}|<0.9\text{ GeV}$. For each track providing good TOF information we calculated the square of the mass of the particle (m_{TOF}^2) from the measured track length, momentum and TOF value. Each event had to contain at least one track with $m_{\text{TOF}}^2>0.1\text{ GeV}^2$. These tracks are referred to as TOF tracks. Events containing tracks

with $m_{\text{TOF}}^2>0.6\text{ GeV}^2$ were rejected to suppress background from events with protons. A sample of 1,412 events survived these selection criteria.

To select events with exactly one charged kaon in the final state we calculated for each TOF track three Gaussian weights W_π , W_K and W_p from the difference between measured TOF and hypothetical TOF (derived from momentum and track length) under the assumption that the track originated from a pion, kaon or proton, respectively. This was done using the formula ($n=\pi, K, p$)

$$W_n=\exp(-(t_{\text{meas}}-t_n)^2/2\sigma^2) \quad (4)$$

where t_{meas} is the measured TOF, t_n the expected TOF under particle hypothesis n and σ the r.m.s. time resolution of the TOF measurement. The weights were normalized by demanding the sum over the weights for a given track to be unity. In this normalisation we accounted for the relative particle fractions. The ratio between π , K and p was estimated to be $\pi:K:p\approx 100:4:3$. The track with the greatest kaon weight W_K had to have $W_K>0.5$. This track was assumed to be the kaon. The product of the kaon weights of the kaon track and any other track X had to be $W_K(K)\cdot W_K(X)<0.25$ if both tracks were oppositely charged in order to suppress contributions from events with charged kaon pairs. The tracks not identified as the kaon were assumed to be pions. The measured TOF for the kaon track had to be consistent with the kaon hypothesis within $\pm 3\sigma$. For the events, where one kaon is identified as described above, the invariant masses of both possi-

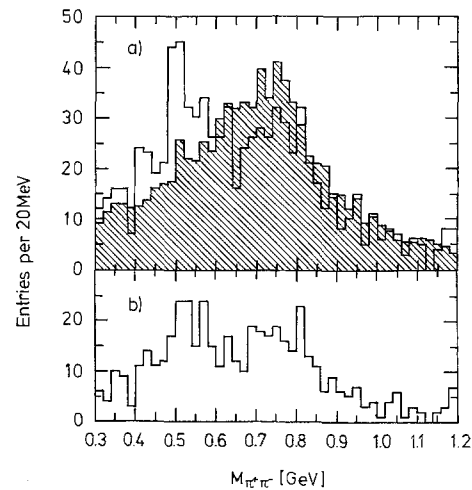


Fig. 4. **a** Invariant mass of both possible $\pi^+\pi^-$ combinations before the cut in $|\sum \mathbf{p}_i|$ if one kaon is identified by the TOF analysis (unshaded histogram) or if one track is taken at random as the kaon (shaded histogram); (2 entries per event). **b** Events of the unshaded histogram in **a**) after the cut in $|\sum \mathbf{p}_i|$ (2 entries per event)

ble $\pi^+\pi^-$ combinations are plotted in Fig. 4a (unshaded histogram; 2 entries per event). This histogram shows a clear signal at the K_S^0 mass. For comparison the shaded histogram in Fig. 4a shows the invariant masses of unlike charge combinations of tracks if no TOF analysis was performed and one track was taken at random as the kaon. In this case there is very little indication of K_S^0 production.

To select fully reconstructed events we demanded the sum of the transverse momenta to be $|\sum \mathbf{p}_t| \leq 0.120$ GeV. This cut effectively restricts background from non-exclusive final states. After these cuts, 249 events were left. For these events, Fig. 4b shows the invariant masses of both possible $\pi^+\pi^-$ combinations (2 entries per event). Here the enhancement in the region of the K_S^0 is less prominent than in the unshaded histogram in Fig. 4a.

The number of candidate events for the reaction $\gamma\gamma \rightarrow K^\pm K_S^0 \pi^\mp$ was determined by demanding at least one $\pi^+\pi^-$ combination in the K^0 mass region defined as a band of width ± 0.016 GeV around the nominal K^0 mass. This corresponds to $\pm 2\sigma$ in the K_S^0 mass resolution of the detector. With this K^0 requirement, 36 events remain. The background is determined from the $\pi^+\pi^-$ combinations falling in sidebands above and below the K^0 mass each of width ± 0.016 GeV. From this procedure a background of 23.5 events not containing a K_S^0 is determined. After subtraction of this background 12.5 ± 6.9 events are left. There still remains background from events with misidentified charged kaons and events with undetected particles. In Fig. 5a we plot the yield of $K^\pm K_S^0 \pi^\mp$ candidate events versus their measured invariant mass. For these events we compare in Fig. 5b the $|\sum \mathbf{p}_t|^2$ distribution with a prediction from a Monte-Carlo simulation of the process (3). No significant enhancement at small values of $|\sum \mathbf{p}_t|^2$ is observed, and thus no indication for exclusive $K^\pm K_S^0 \pi^\mp$ production.

Hence we derived upper limits on the cross section $\sigma(\gamma\gamma \rightarrow K^+ \bar{K}^0 \pi^-$ or $K^- K^0 \pi^+)$. They were obtained using the same Monte-Carlo method as in the analysis of reaction (2) including this time the simulation of the TOF counters in the detector simulation. The $K\bar{K}\pi$ final state was generated according to phase space. Fig. 6 shows the upper limits on the cross section $\sigma(\gamma\gamma \rightarrow K^+ \bar{K}^0 \pi^-$ or $K^- K^0 \pi^+)$ for three different $W_{\gamma\gamma}$ bins (95% C.L.). The values are corrected for K_L^0 production and the unseen decay modes of the K_S^0 . A systematic error of 15% has been included in the computation of the upper limits.

We also set limits on the formation of the final states $K\bar{K}\pi$ via resonances with even C-parity, such as the $\iota(1440)$ and the $\eta_c(2980)$. The Particle Data

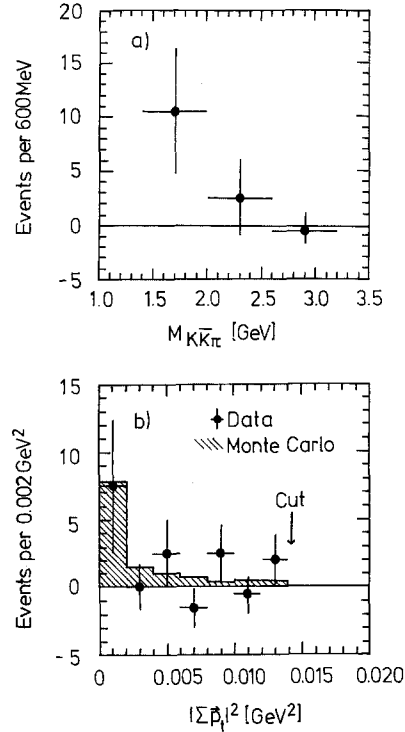


Fig. 5. a) Yield of candidate events for $\gamma\gamma \rightarrow K^\pm K_S^0 \pi^\mp$ as a function of the measured invariant mass (not corrected for background events with misidentified K^\pm or additional undetected particles). b) $|\sum \mathbf{p}_t|^2$ distribution of the events in a) (data points) compared to a Monte-Carlo simulation of $K^\pm K_S^0 \pi^\mp$ production (histogram)

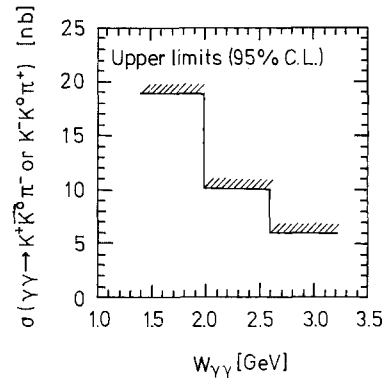


Fig. 6. Upper limit on the cross section $\sigma(\gamma\gamma \rightarrow K^+ \bar{K}^0 \pi^-$ or $K^- K^0 \pi^+)$

Group gives for the mass, width and spin-parity of the $\iota(1440)$: $m = (1.440 \pm 0.010)$ GeV, $\Gamma = (0.076 \pm 0.010)$ GeV, and $J^P = 0^-$, respectively [12]. The Mark III group finds in a high statistics experiment somewhat different values, $m_\iota = (1.456 \pm 0.010)$ GeV, and $\Gamma_\iota = (0.095 \pm 0.010)$ GeV [6]. In deriving an upper limit on $\iota(1440)$ production we took both sets of parameters into account. Applying the more restrictive cut $|\sum \mathbf{p}_t| \leq 0.100$ GeV two events are found in

the $W_{\gamma\gamma}$ range between 1.300 GeV and 1.550 GeV. These events lead to an upper limit on the product of the two-photon width of the $\iota(1440)$ times the branching ratio into the $K\bar{K}\pi$ final states of $\Gamma(\gamma\gamma\rightarrow\iota(1440))\cdot\text{BR}(\iota(1440)\rightarrow K\bar{K}\pi)<2.2\text{ keV}$ at 95% C.L. where the branching ratio accounts for all charge modes of $K\bar{K}\pi$ according to the decomposition of an isoscalar particle. This upper limit includes a systematic error in the acceptance calculation of 20%.

In case of the charmonium state $\eta_c(2980)$ which has $J^P=0^-$ [12] no event was found in a range of $\pm 0.110\text{ GeV}$ around the nominal resonance mass, which corresponds to a $\pm 2\sigma$ interval of the mass resolution of the detector in the $\eta_c(2980)$ range. From this we derived an upper limit (95% C.L.) on the product of the $\gamma\gamma$ width times the branching ratio into the $K\bar{K}\pi$ final states of $\Gamma(\gamma\gamma\rightarrow\eta_c(2980))\cdot\text{BR}(\eta_c(2980)\rightarrow K\bar{K}\pi)<4.4\text{ keV}$.

5. Discussion and Summary

We have measured the total cross section for two-photon production of neutral kaon pairs $\sigma(\gamma\gamma\rightarrow K^0\bar{K}^0)$. The observed enhancement near threshold may indicate some contribution from scalar resonances near threshold such as $S^*(975)$ and $\delta(980)$ although statistics do not allow definite conclusions. The angular distribution of the events near threshold is consistent with S-wave production of $K^0\bar{K}^0$ pairs. Note that in the charged kaon channel, $\gamma\gamma\rightarrow K^+K^-$, the direct coupling of the photons to the charge of the mesons could produce a threshold enhancement, which is, however, not expected in the neutral kaon channel.

The $W_{\gamma\gamma}$ region between about 1.2 and 1.6 GeV is well described by an interfering sum of the three resonances $f(1270)$, $A_2(1320)$, and $f'(1525)$ using previously determined $\gamma\gamma$ couplings. While the $f'(1525)$ is clearly seen in the cross section, the $f(1270)$ and the $A_2(1320)$ are not seen in the neutral kaon final state. This can be explained by destructive interference of their Breit-Wigner resonance amplitudes.

For the $\Theta(1700)$ we derive an upper limit (95% C.L.) on the product of the $\gamma\gamma$ width times the branching ratio into the $K\bar{K}$ final states of $\Gamma(\gamma\gamma\rightarrow\Theta(1700))\cdot\text{BR}(\Theta(1700)\rightarrow K\bar{K})<0.28\text{ keV}$. This value holds for spin $J=2$ and helicity $\lambda=2$ assignments. If $\lambda=0$ is assumed, the upper limit increases by a factor of two. In the $K\bar{K}$ spectrum observed in radiative J/ψ decays, $J/\psi\rightarrow\gamma K\bar{K}$, the $\Theta(1700)$ is the most prominent signal. The comparison of this spectrum with the one obtained in $\gamma\gamma$ reactions, where

no $\Theta(1700)$ signal is visible (although the $f'(1525)$ is observed), has been taken as a further indication for the glueball character of the $\Theta(1700)$ [13].

For the $h(2030)$ we find $\Gamma(\gamma\gamma\rightarrow h(2030))\cdot\text{BR}(h(2030)\rightarrow K\bar{K})<0.29\text{ keV}$. This upper limit is derived for spin $J=4$ and holds for helicity $\lambda=0$ and $\lambda=2$ assumptions. Recently the JADE collaboration has given a preliminary upper limit on the $\gamma\gamma$ width of the $h(2030)$ by analysing the $\pi^0\pi^0$ final state [14]. Since the branching ratio into $\pi\pi$ is much larger than into $K\bar{K}$ [12] their limit is much more stringent.

For the $\xi(2220)$ we get $\Gamma(\gamma\gamma\rightarrow\xi(2220))\cdot\text{BR}(\xi(2220)\rightarrow K\bar{K})\cdot(2J+1)<1.0\text{ keV}$ which holds for $J=0$ or $J=2$ with helicity $\lambda=0$ and $\lambda=2$.

No clear evidence for two-photon production of $K\bar{K}\pi$ was found. Thus we derived upper limits on the cross section for the reaction $\gamma\gamma\rightarrow K^+K^0\pi^-$ or $K^-K^0\pi^+$.

An upper limit (95% C.L.) was also obtained on the product of the $\gamma\gamma$ width times the branching ratio into the $K\bar{K}\pi$ final states for the $\iota(1440)$ of $\Gamma(\gamma\gamma\rightarrow\iota(1440))\cdot\text{BR}(\iota(1440)\rightarrow K\bar{K}\pi)<2.2\text{ keV}$. A less stringent limit has been obtained before by the Mark II collaboration [15]. The classification of the $\iota(1440)$ which has been discovered in radiative J/ψ decays ($J/\psi\rightarrow\gamma\iota$) [5] is controversial (see e.g. references in [3]). Due to its large production rate in this ‘glueball-favoured’ channel the $\iota(1440)$ is thought to be a glueball candidate. In this case one would naively expect a small $\gamma\gamma$ coupling due to the suppression by an extra quark loop. However, there are also models predicting a relatively large $\gamma\gamma$ coupling due to mixing with $q\bar{q}$ states or due to the axial anomaly in the pseudoscalar sector [16]. Thus predictions for $\Gamma_{\gamma\gamma}(\iota(1440))$ range from 0.07 to about 50 keV [17]. Assuming that $\iota(1440)\rightarrow K\bar{K}\pi$ is the dominant decay mode some of the models are excluded by our data.

In case of the $\eta_c(2980)$ we obtained an upper limit on the product of the two-photon width times the branching ratio into the $K\bar{K}\pi$ final states of $\Gamma(\gamma\gamma\rightarrow\eta_c(2980))\cdot\text{BR}(\eta_c(2980)\rightarrow K\bar{K}\pi)<4.4\text{ keV}$. Predictions of the $\gamma\gamma$ width of the $\eta_c(2980)$ range between about 1 and 6 keV. Thus the derived upper limit is not very stringent since the branching ratio $\text{BR}(\eta_c(2980)\rightarrow K\bar{K}\pi)$ is measured to be $14^{+7}_{-6}\%$ [12].

Acknowledgements. We gratefully acknowledge the support by the DESY directorate, the PETRA machine group and the DESY computer centre. Those of us from abroad wish to thank the DESY directorate for the hospitality extended to us while working at DESY. We thank Dr. N. Wermes for discussions on the Mark III results.

References

1. H.W. Atherton et al.: Phys. Lett. **158B**, 81 (1985)
2. A. Cordier: Proceedings of the VIth International Workshop on Photon Photon Collisions, Ed. R.L. Lander, Lake Tahoe (1984)
3. for a review see e.g.: H. Kolanoski: Springer Tracts in Modern Physics, Vol. 105. Berlin, Heidelberg, New York: Springer 1984
4. B.A.Li, K.F. Liu: Phys. Lett. **118B**, 435 (1982); Erratum, Phys. Lett. **124B**, 550 (1983); N.N. Achasov, S.A. Devyanin, G.N. Shestakov: Phys. Lett. **108B**, 134 (1982); Z. Phys. C – Particles and Fields **16**, 55 (1982)
5. D.L. Scharre et al.: Phys. Lett. **97B**, 329 (1980); C. Edwards et al.: Phys. Rev. Lett. **49**, 259 (1982); Erratum, Phys. Rev. Lett. **50**, 219 (1983)
6. C. Edwards et al.: Phys. Rev. Lett. **48**, 458 (1982); E. Bloom: Proceedings of the XXIst International Conference on High Energy Physics, Eds. P. Petiau, M. Porneuf, Paris (1982); for a recent summary see: A. Odian, Presentation at the Meeting of the Division of Particles and Fields of the American Physical Society, Santa Fe (1984), SLAC-PUB-3589 (1985)
7. K.F. Einsweiler: Proceedings of the International Europhysics Conference on High Energy Physics, Eds. J. Guy, C. Costain: Brighton (1983); N. Wermes: Proceedings of the XIXth Rencontre de Moriond on New Particle Production, Ed. J. Tran Thanh Van: La Plagne (1984); W. Toki: Invited talk presented at the XIIIth SLAC Summer Institute on Particle Physics (1985), to appear in the Proceedings
8. TASSO Collab., R. Brandelik et al.: Z. Phys. C – Particles and Fields **4**, 87 (1980); Phys. Lett. **83B**, 261 (1979)
9. V.M. Budnev, I.F. Ginzburg, G.V. Meledin, V.G. Serbo: Phys. Rep. **15**, 181 (1975)
10. TASSO Collab., M. Althoff et al.: Phys. Lett. **121B**, 216 (1982)
11. D. Faiman, H.J. Lipkin, H.R. Rubinstein: Phys. Lett. **59B**, 269 (1975); L. Köpke: Ph. D. Thesis, Bonn University BN-IR-83-16 (1983)
12. Particle Data Group: Rev. Mod. Phys. **56**, 2(II) (1984)
13. M. Chanowitz: Proceedings of the VIth International Workshop on Photon Photon Collisions, Ed. R.L. Lander: Lake Tahoe (1984); A.M. Zaitsev: Proceedings of the XXIInd International Conference on High Energy Physics, Eds. A. Meyer, E. Wieczorek: Vol. II, Leipzig (1984)
14. J.E. Olsson: Proceedings on the Vth International Workshop on Photon Photon Collisions, Aachen (1983). Lecture Notes in Physics, Vol. 191, Ed. Ch. Berger. Berlin, Heidelberg, New York: Springer 1983
15. P. Jenni et al.: Phys. Rev. **D27**, 1031 (1983)
16. K.A. Milton, W.F. Palmer, S.S. Pinsky: Proceedings of the XVIIth Rencontre de Moriond, Vol. II, Ed. J. Tran Thanh Van: Les Arcs (1982)
17. K. Ishikawa: Phys. Rev. Lett. **46**, 978 (1981); T. Teshima, S. Oneda: Phys. Lett. **123B**, 455 (1983); Phys. Rev. **D27**, 1551 (1983); C. Rosenzweig, A. Salomone, J. Schechter: Phys. Rev. **D24**, 2545 (1981); S. Iwao: Lett. Nuovo Cimento **35**, 481 (1982); H. Goldberg: Phys. Rev. **D22**, 2286 (1980)